

Ferroelastic Phases in $\text{Pb}_3(\text{PO}_4)_2\text{--Pb}_3(\text{AsO}_4)_2$; X-ray and Optical Experiments

BY U. BISMAYER AND E. SALJE

*Mineralogisches Institut der Universität Hannover, Welfengarten 1, 3000 Hannover,
Federal Republic of Germany*

(Received 16 June 1980; accepted 18 September 1980)

Abstract

Mixed crystals $\text{Pb}_3(\text{PO}_4)_2\text{--Pb}_3(\text{AsO}_4)_2$ are ferroelastic at low temperatures. The phase diagram contains three different phases a (paraelastic), b and c (both ferroelastic). The transformation a–b is first order for $\text{Pb}_3(\text{PO}_4)_2$ and approaches second-order behaviour with increasing As content. The spontaneous strains and the birefringence follow approximately a Curie–Weiss law, with a corresponding order-parameter exponent $\beta = \frac{1}{4}$. The mutual high-temperature phases give diffuse X-ray reflections due to inelastic scattering. The soft-mode model is discussed for these results.

Introduction

Lead phosphate, $\text{Pb}_3(\text{PO}_4)_2$, is a well-known ferroelastic material with a ferroelastic phase transformation not accompanied by dielectric singularities (Brixner, Bierstedt & Jaep, 1973). The ferroelastic hysteresis was determined by Salje & Hoppmann (1976), the temperature dependence of the critical stress by von Hodenberg & Salje (1977). It was found that the critical stress as well as the spontaneous strains (Guimaraes, 1979*a,b*) follow a Curie–Weiss law up to ca 430 K. At higher temperatures a crossover to a regime with different critical parameters occurs with a phase transition point at 453 K.

In the paraelastic phase, Joffrin, Benoit, Deschamps & Lambert (1977) observed weak and diffuse X-ray reflections not compatible with the space group $R\bar{3}m$ of the paraelastic phase. These reflections were interpreted as being due to monoclinic microdomains because they could be indexed according to the monoclinic symmetry ($C2/c$) of the ferroelastic phase. The size of the microdomains was estimated from the diffuse broadening of the reflections as ca 5 to 36 nm depending on temperature and pressure (Decker, Petersen, Debray & Lambert, 1979). According to three equivalent domain orientations, three sets of superreflections with the same intensities were expected. In fact, all these reflections have been observed by Joffrin *et al.* (1977), which seems to confirm the microdomain model.

Whereas this model dominated the interpretation of

some experimental results, other authors like Torres (1975) and Salje & Iishi (1977) stressed the aspect of a critical-mode behaviour. It was shown that, if a critical phonon condenses at the L point (Torres, 1975) on the surface of the Brillouin zone of the paraphase, the subsequent structural transformation is in accordance with the observed transformation. Salje & Iishi (1977) gave evidence for such weakening of phonon branches in terms of the lattice dynamics of the paraphase. Unfortunately, the results of infrared and Raman experiments could not prove this model, although the softening of one critical phonon branch was observed by Benoit (1976) and Benoit & Chapelle (1974) at higher frequencies. Joffrin, Benoit, Currant & Lambert (1979) have described their results of inelastic neutron scattering. At least one critical mode near $\omega = 0$ was found whose character is compatible with the structural transformation at the transition point. Furthermore, this mode is heavily overdamped with zero-frequency scattering intensities observable in X-ray experiments. Therefore, these authors attribute the X-ray superreflections to the appearance of the soft mode and *not* to the existence of microdomains.

According to Salje & Iishi (1977), the critical behaviour of the corresponding phonon branches is mainly due to the ionic part of the Pb–O interaction and partly to Pb–Pb coupling. Hence, in a first approximation, ferroelasticity should also be found if the tetrahedrally coordinated P is changed to other elements like V or As. It has been shown that most $\text{Pb}_3(\text{P}_{1-x}\text{V}_x\text{O}_4)_2$ mixed crystals are ferroelastic with a behaviour similar to $\text{Pb}_3(\text{PO}_4)_2$. Unfortunately, the ferroelastic state could not be followed for the whole series of chemical compositions because the transition temperature near $x = 0.5$ is extremely low. Furthermore, in $\text{Pb}_3(\text{VO}_4)_2$ the ferroelastic transformation takes place at temperatures close to another antiferroelectric transition (von Hodenberg & Salje, 1977).

In this paper we present the results of optical and X-ray experiments on $\text{Pb}_3(\text{P}_{1-x}\text{As}_x\text{O}_4)_2$ in which ferroelasticity remains observable for all chemical compositions and is uncoupled with dielectric anomalies. These results are compared with those of the lattice dynamics of these compounds which will be described in a parallel paper.

Crystal growth

Starting materials for crystal growth were prepared with PbO (Merck Art. 7401), $(\text{NH}_4)_2\text{H}_2\text{PO}_4$ (Merck Art. 1126) and $3\text{As}_2\text{O}_5 \cdot 5\text{H}_2\text{O}$ (Merck Art. 114). The preparation of $\text{Pb}_3(\text{PO}_4)_2$ was described by Torres, Aubrée & Brandou (1974). To obtain $\text{Pb}_3(\text{AsO}_4)_2$, PbO and $3\text{As}_2\text{O}_5 \cdot 5\text{H}_2\text{O}$ were thoroughly mixed and drained at 720 K for 8 h. Then the mixture was heated to 1370 K in a closed Al_2O_3 crucible. The molten $\text{Pb}_3(\text{AsO}_4)_2$ was slowly cooled to room temperature. For growing the mixed crystals, $\text{Pb}_3(\text{PO}_4)_2$ and $\text{Pb}_3(\text{AsO}_4)_2$ were pulverized and then mixed in the desired proportions. Crystals were grown by the Czochralski technique. The prepared powders were melted in a Pt crucible of 35 mm diameter and 37 mm height imbedded in MgO powder. The crucible was in a water-cooled quartz cylinder fitted inside the work coil of a 10 kW, 600 kHz, r.f. generator. The temperature was governed by a thermocouple and a powder regulator. The pull rate of the crystals was 1 mm h^{-1} , the rotation rate 8 r min^{-1} .

Crystal habit and lattice constants

The crystals of P-rich compounds are slightly yellowish, those with high As content are colourless. All crystals exhibit a cleavage plane parallel to the pull direction. The crystal boules were cut into parallelepipeds for further experiments. For examination of lattice constants powders were prepared from the melt. The chemical compositions of the powder probes are found to be better defined than those of the single crystals because no noticeable chemical decomposition by evaporation of the highly volatile components takes place during the short time of melting in a covered crucible. The lattice constants were determined with a Guinier focusing camera and $\text{Cu } K\alpha_1$ radiation. Si ($a_0 = 0.5406 \text{ nm}$) served as internal standard. The d values of the 25–30 sharpest lines were measured and indexed according to monoclinic or trigonal symmetry. None of the weak and diffuse reflections of the residual phases

has been taken into account for this determination of the lattice constants. The results are listed in Table 1. Three different phases can be distinguished:

(a) the trigonal phase with space group $R\bar{3}m$ ($0.36 < x < 0.65$);

(b) the monoclinic phase with space group $C2/c$ for the phosphate-rich probes ($0 \leq x \leq 0.36$) and for As-rich probes ($0.65 \leq x \leq 0.96$);

(c) the monoclinic phase with space group $P2_1/c$ for the nearly pure lead arsenate ($0.96 < x \leq 1$).

In the literature, the phase a is labelled β , the phase b is labelled α . We suggest another notation because in different systems of mixed crystals several phases occur at temperatures below the stability range of phase b(α) but none above a(β). It seems more convenient to indicate these phases by c, d ... than by $\alpha_1, \alpha_2 \dots$. As will be described later, the phases b and c are ferroelastic, phase a paraelastic.

The transformation of the unit cells for the two first phases a and b has been described (Joffrin *et al.*, 1977; von Hodenberg, 1974). The relationships between the respective lattice constants are:

$$\begin{aligned} a_a &= b_b & a_b &= \frac{1}{3}(4c_a^2 + 3a_a^2)^{1/2} \\ b_a &= \frac{1}{2}(b_b^2 + c_b^2)^{1/2} & b_b &= a_a \\ c_a &= \frac{3}{2}(a_b^2 - \frac{1}{9}c_b^2)^{1/2} & c_b &= \sqrt{3}a_a. \end{aligned}$$

Here, for convenience, the hexagonal setting has been chosen for phase a. The relationships between the lattice constants of the two monoclinic phases b and c are:

$$\begin{aligned} a_b &= [4a_c^2 + c_c^2 - 4a_c c_c \cos(180 - \beta_c)]^{1/2} \\ b_b &= b_c \\ c_b &= c_c. \end{aligned}$$

The geometrical arrangement of the unit cells is shown in Fig. 1. With the given relations, the lattice constants of the different phases have been related to the unit cell of the monoclinic phase b and the trigonal

Table 1. Lattice constants of $\text{Pb}_3(\text{P}_{1-x}\text{As}_x\text{O}_4)_2$

	a (Å)	b (Å)	c (Å)	β (°)	Space group
$x = 0.0$	13.813 (5)	5.693 (1)	9.436 (2)	102.33 (2)	$C2/c$
0.10	13.836 (4)	5.705 (1)	9.475 (2)	102.45 (2)	$C2/c$
0.20	13.852 (5)	5.712 (1)	9.518 (3)	102.43 (3)	$C2/c$
0.30	13.882 (7)	5.709 (2)	9.580 (5)	102.70 (5)	$C2/c$
0.40	5.626 (4)	5.626 (4)	2.372 (13)	hexagonal	$R\bar{3}m$
0.50	5.646 (2)	5.646 (2)	20.375 (5)	hexagonal	$R\bar{3}m$
0.63	5.676 (3)	5.676 (3)	20.392 (7)	hexagonal	$R\bar{3}m$
0.69	13.939 (6)	5.749 (5)	9.663 (10)	102.99 (9)	$C2/c$
0.82	13.962 (4)	5.793 (2)	9.740 (4)	102.99 (4)	$C2/c$
0.90	13.960 (4)	5.822 (2)	9.792 (4)	102.86 (3)	$C2/c$
0.97	13.971 (4)	5.829 (2)	9.805 (4)	102.90 (3)	$C2/c$
1.0 (at 293 K)	7.536 (3)	6.029 (2)	9.509 (4)	115.15 (3)	$P2_1/c$
1.0 (at 333 K)	14.005 (3)	5.828 (1)	9.839 (3)	103.05 (2)	$C2/c$
1.0 (at 593 K)	5.749 (1)	5.749 (1)	20.556 (7)	hexagonal	$R\bar{3}m$

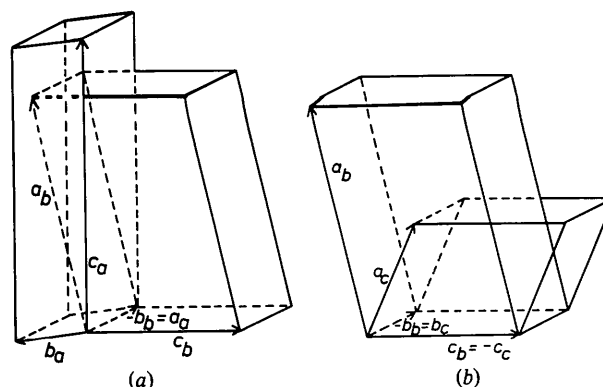


Fig. 1. Geometrical relations of the unit cells (a) a-b and (b) b-c.

phase a. In this way the dependence of the lattice constants on the chemical composition can be demonstrated (Figs. 2 and 3).

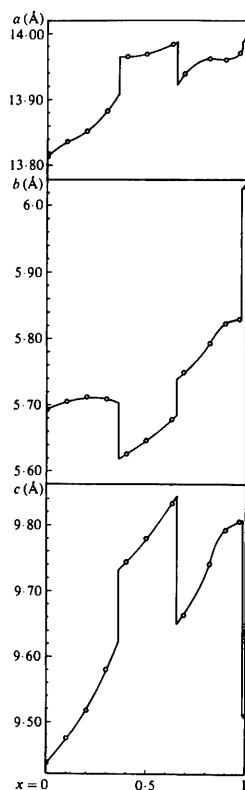


Fig. 2. Dependence of monoclinic cell parameters on chemical composition.

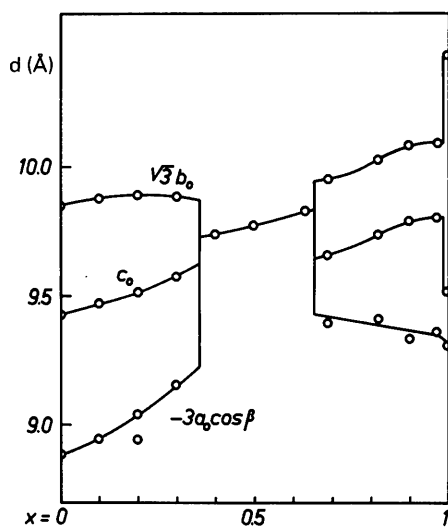


Fig. 3. Parameters $\sqrt{3}b_0$, c_0 , and $-3a_0 \cos \beta$ versus chemical composition.

High-temperature lattice constants of $\text{Pb}_3(\text{AsO}_4)_2$

The monoclinic phase appears at room temperature as for compounds with low P content (<4%). At high temperatures this phase transforms to the monoclinic phase b and ultimately to the trigonal modification. The lattice constants are listed in Table 2 and shown with respect to the monoclinic unit cell b in Fig. 4. Again,

Table 2. Lattice constants of $\text{Pb}_3(\text{AsO}_4)_2$ for various temperatures as determined from reflections 020, 113, 711, 622, 224, 515, 133 and 206

The monoclinic axes have been chosen for both phases a ($R\bar{3}m$, above 563 K) and b ($C2/c$, below 563 K).

T (K)	a (Å)	b (Å)	c (Å)	β (°)
328	13.994 (9)	5.827 (4)	9.842 (8)	102.96 (5)
333	14.005 (3)	5.828 (1)	9.839 (3)	103.05 (2)
353	14.007 (11)	5.814 (5)	9.859 (11)	103.07 (7)
373	14.015 (6)	5.803 (3)	9.859 (6)	103.09 (4)
403	14.024 (4)	5.795 (2)	9.877 (4)	103.22 (2)
433	14.033 (5)	5.791 (2)	9.900 (5)	103.45 (3)
463	14.040 (15)	5.775 (6)	9.922 (15)	103.46 (9)
473	14.048 (14)	5.769 (6)	9.930 (14)	103.45 (9)
483	14.052 (7)	5.761 (3)	9.934 (7)	103.43 (5)
498	14.061 (5)	5.756 (2)	9.944 (5)	103.52 (3)
523	14.072 (2)	5.752 (1)	9.951 (2)	103.58 (2)
553	14.092 (9)	5.750 (4)	9.946 (9)	103.59 (6)
563	14.092 (8)	5.747 (2)	9.951 (5)	103.62 (4)
573	14.091 (6)	5.748 (2)	9.953 (4)	103.62 (3)
593	14.100 (4)	5.749 (1)	9.955 (2)	103.62 (2)
611	14.107 (4)	5.751 (1)	9.959 (2)	103.61 (2)
623	14.111 (7)	5.750 (2)	9.959 (4)	103.61 (4)
633	14.108 (3)	5.752 (1)	9.961 (2)	103.61 (2)
643	14.111 (7)	5.752 (2)	9.959 (4)	103.61 (4)
653	14.111 (7)	5.752 (2)	9.959 (4)	103.61 (4)

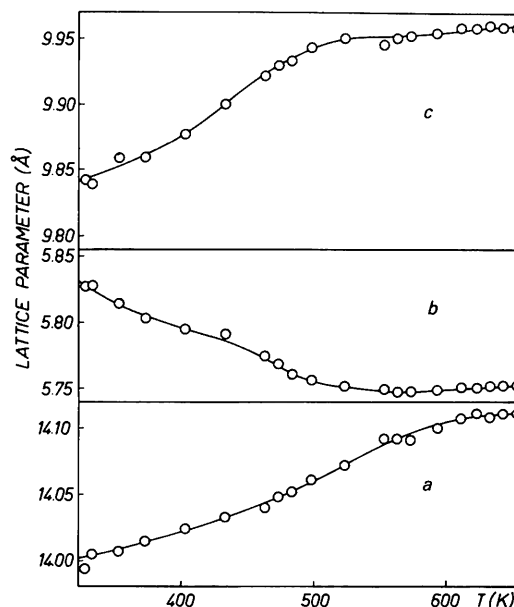


Fig. 4. Temperature dependence of lattice constants of $\text{Pb}_3(\text{AsO}_4)_2$.

just the sharp and intense reflections have been used for the determination of the lattice constants, so that effects of superstructures have been neglected.

In both monoclinic phases, the b lattice constant shrinks with increasing temperature in accordance with results from $\text{Pb}_3(\text{PO}_4)_2$ (Guimaraes, 1979*b*). The lattice constants a and c exhibit similar thermal expansion. The phase transformation $a \rightarrow b$ at 333 K appears as an abrupt change of the lattice constants; this transformation is of first order. The transformation $b \rightarrow c$ near 563 K is almost second order.

The spontaneous deformation of the ferroelastic phases

The tensor components of the spontaneous strain of the species $3mF2/m$ are ϵ_{11} and ϵ_{13} (Toledano, Pateau, Primot, Aubrée & Morin, 1975) with

$$\epsilon_{11} = (c_b/\sqrt{3} - b_b)/2b_b,$$

$$\epsilon_{13} = (c_b + 3a_b \cos \beta)/(6a_b \sin \beta).$$

The scalar spontaneous strain is given by (Aizu, 1970)

$$\epsilon_s = [2\epsilon_{11}^2 + 2\epsilon_{13}^2]^{1/2}.$$

These parameters have been determined for $\text{Pb}_3(\text{PO}_4)_2$ by Guimaraes (1979*a*) who found that ϵ_s follows a Curie-Weiss law up to near 430 K and a Curie temperature *below* the transition temperature $b \rightarrow a$. At 430 K a crossover to a first-order regime takes place, valid up to the transition point at 453 K.

Similar results were obtained for the mixed crystals. In Fig. 5 the spontaneous strains are given for $\text{Pb}_3(\text{AsO}_4)_2$. Again, the parameter ϵ_s follows, to a

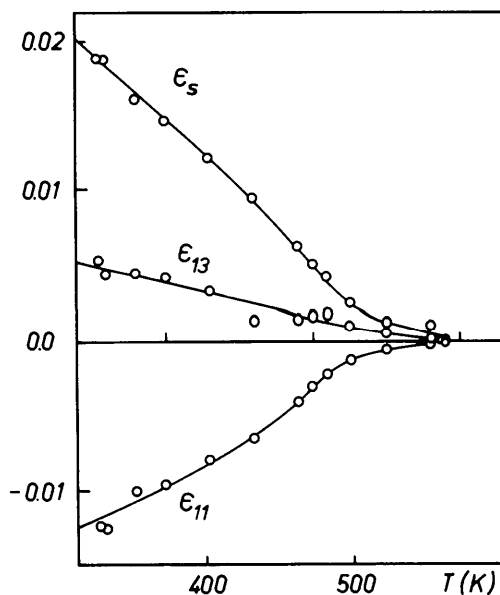


Fig. 5. Spontaneous strains of $\text{Pb}_3(\text{AsO}_4)_2$ versus temperature.

reasonable approximation, a critical behaviour with a Curie temperature of 508 K. Deviations at low temperatures are due to the influence of the $b \rightarrow c$ transformation at 333 K.

At 493 K a crossover occurs to an extended regime with reduced slopes $\partial\epsilon_s/\partial T$. This regime remains valid up to the transformation point near 563 K. In contrast to $\text{Pb}_3(\text{PO}_4)_2$ the phase transformation is approximately second order. The Curie temperature of the first regime (508 K) is as much as 55 K below the phase transformation point. In $\text{Pb}_3(\text{PO}_4)_2$ this transition range is much smaller, namely *ca* 20 K.

The diffuse X-ray reflections of the single crystals

As Joffrin *et al.* (1977) pointed out, the structural transformation $b \rightarrow a$ of $\text{Pb}_3(\text{PO}_4)_2$ is always accompanied by the appearance of diffuse superreflections in the paraelastic phase. This effect is due to the overdamped critical phonon and is therefore directly correlated with the ferroelastic transformation (Joffrin *et al.*, 1979; Salje & Iishi, 1977).

In $\text{Pb}_3(\text{P}_{1-x}\text{As}_x\text{O}_4)_2$ the corresponding diffuse reflections have been observed for all chemical compositions. In Fig. 6(*a*) the precession film of $\text{Pb}_3(\text{P}_{0.48}\text{As}_{0.52}\text{O}_4)_2$ is given for room temperature. The indices of the reflections are summarized in Fig. 7. The superreflections are more intense and less diffuse than in $\text{Pb}_3(\text{PO}_4)_2$ and can easily be followed up to temperatures *ca* 70 K above the ferroelastic transition point. With increasing As content, the phase transformation becomes more and more second order and, consequently, the transition between the intensities of the allowed reflection in phase b and the corresponding diffuse spots in phase a is less abrupt in compounds with high x values. For $\text{Pb}_3(\text{AsO}_4)_2$ the phase transformation is very smooth from the observation of the temperature dependence of the 021 reflection in Fig. 8.

During the transformation $c \rightarrow b$, some additional reflections of phase c are symmetry-extinct in phase b . Nevertheless, diffuse spots are observable (Fig. 5*b*) and must be indexed accordingly by half integers (*e.g.* $\frac{1}{2}\frac{1}{2}\frac{1}{2}$). With increasing temperature, their intensities reduce continuously. Above 643 K [$\text{Pb}_3(\text{AsO}_4)_2$] none of these reflections could be observed even for an exposure of one week. It seems unlikely that this effect is due to macroscopic parts of the crystal which do not transform their structure, for the following reasons:

- (1) the reflections appear in all crystals, even in those which are perfect single crystals from optical examination;
- (2) the reflections show identical intensities for all parts of a large single crystal;
- (3) the reflections are somewhat diffuse and remain observable at temperatures far above the transition point.

It is not yet clear whether these reflections ($c \rightarrow b$) are due to another critical-mode behaviour similar to the transformation $b \rightarrow a$ or due to the appearance of microdomains. Further experiments are planned on this subject.

Macroscopic domain structure

Ferroelastic twinning is expected if the spontaneous strain of the ferroelastic phase is not too large. The

twins are oriented with respect to the pseudosymmetries 2 and m which occur in the paraelastic but not in the ferroelastic form. For the transformation $a \rightarrow b$ two pseudomirror planes, namely $(11\bar{3})_b$ and $(\bar{1}\bar{1}\bar{3})_b$, and the pseudobinary axes $[011]_b$ and $[0\bar{1}\bar{1}]_b$ fulfil this condition. The respective domain patterns have been described by Chabin & Gilletta (1977) who denote the domain walls due to the pseudomirror W wall and those due to a pseudobinary axis W' wall. We henceforth use the same notation.

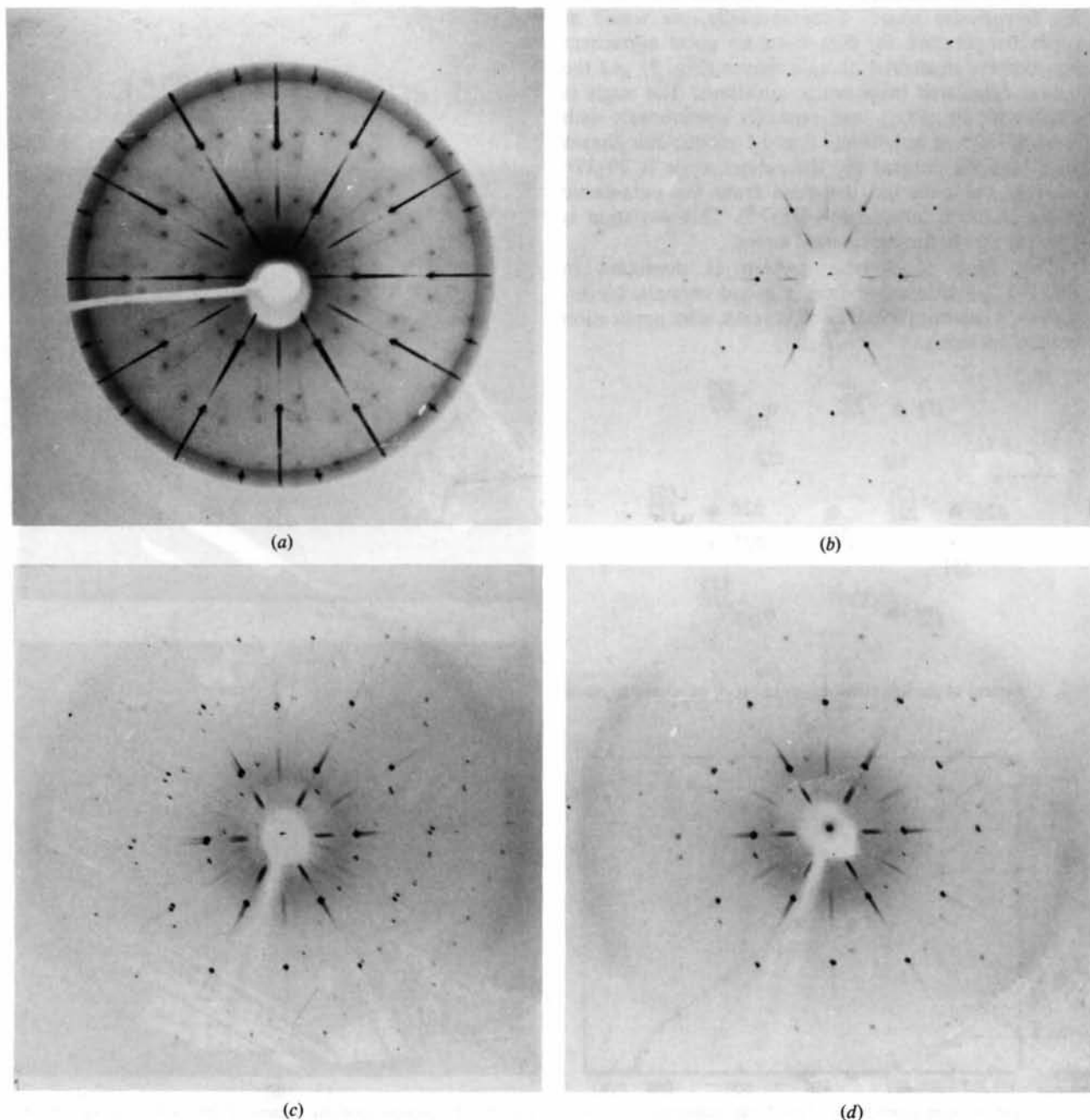


Fig. 6. Zero-layer precession photos of (a) $Pb_3(P_{0.48}As_{0.52}O_4)_2$ at 273 K and $Pb_3(AsO_4)_2$ at (b) 312 K, (c) 343 K and (d) 543 K.

(a) **W walls**

The angle between the cleavage plane (100) and the domain wall is slightly less than 90° and hence the crystal surface (100) appears bent at the trace of the **W** wall on the surface. The angle between the monoclinic binary axis [010] and this trace on the surface (*i.e.* the [031] direction) is

$$\tan \varphi_b = c/3b_b$$

with the monoclinic constants b_b and c_b . This angle is 30° in the paraelastic phase and reduces with increasing ferroelastic strain. Experimentally, we found at room temperature for low x values good agreement between the measured domain angles (Fig. 9) and the values calculated from lattice constants. The angle is 28.92° for $\text{Pb}_3(\text{PO}_4)_2$ and increases continuously with x up to 30° at $x = 0.41$. For the monoclinic phases with high As content the theoretical angle is 29.27° whereas the observed deviation from the paraelastic phase is much larger ($\varphi = 28.1^\circ$). This deviation is possibly due to further internal stress.

This type of domain pattern is dominant in $\text{Pb}_3(\text{PO}_4)_2$ and less common in mixed crystals. Nevertheless, it has been found in all crystals after application of external stress.

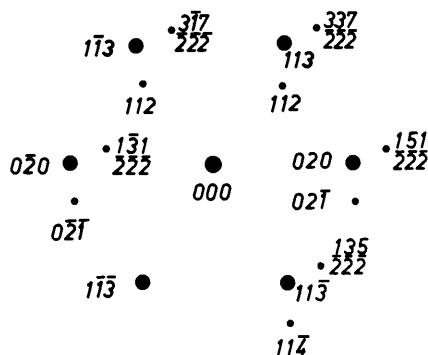


Fig. 7. Indices of the reflections given in Fig. 6 as related to phase b.

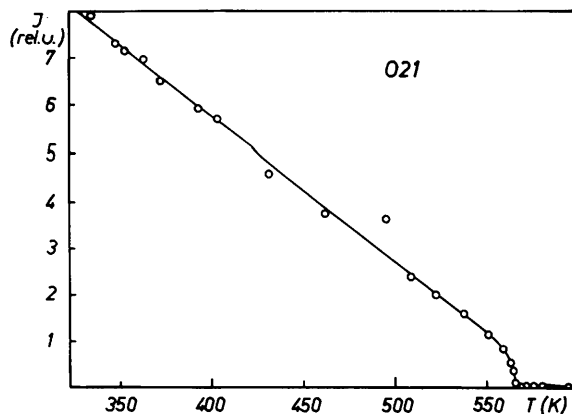


Fig. 8. Temperature dependence of the X-ray scattering intensity of 021_b . This reflection remains observable up to 633 K.

(b) **W' walls**

The **W'** walls are tilted against the normal of the cleavage plane by an angle θ with

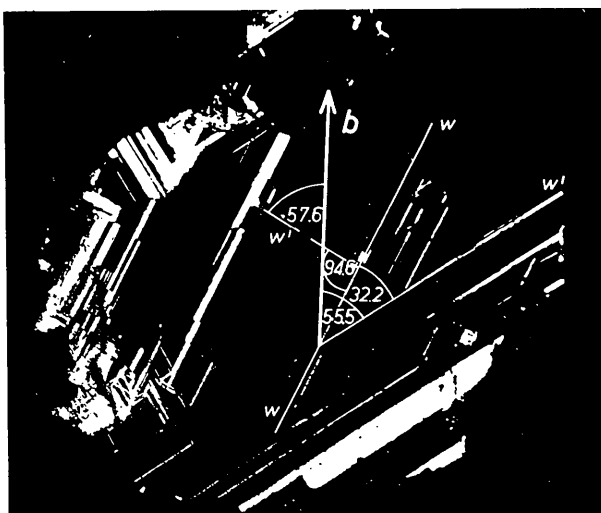
$$\tan \theta = 2\varepsilon_{13}^0 / (\varepsilon_{11}^0 - \varepsilon_{22}^0)$$

and the strain parameters

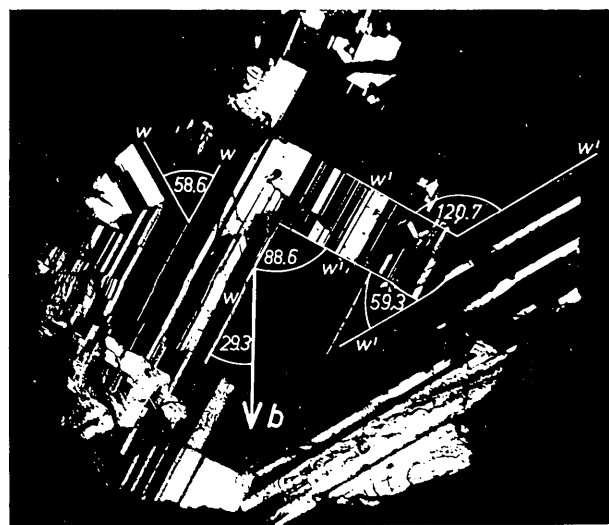
$$\varepsilon_{11}^0 = \frac{\sqrt{3}b_a - c_c}{\sqrt{3}b_a}$$

$$\varepsilon_{22}^0 = \frac{b_a - b_b}{b_b}$$

$$\varepsilon_{13}^0 = \frac{1}{2} \cos \left(\frac{\pi}{2} + \frac{c_b + 3a_b \cos \beta}{3a_b \sin \beta} \right).$$



(a)



(b)

Fig. 9. Microscopic domain pattern of $\text{Pb}_3(\text{AsO}_4)_2$ at (a) 293 K (phase c) and (b) 333 K (phase b).

Therefore, the domain walls appear under the optical microscope as stripes of interference fringes (Chabin & Gilletta, 1977). The inclination angle was found to be $17.5 \pm 2^\circ$ for all mixed crystals.

The angle between the traces of the domain walls on the cleavage plane and the binary axis is determined by

$$\tan \phi' = 3 \tan \phi,$$

which was found to hold for all probes examined. This type of domain appears more frequently in crystals with high As content.

In $\text{Pb}_3(\text{AsO}_4)_2$, phase c, the possible pseudo-symmetries 2 and m show identical traces on the cleavage plane as in phase b because the respective crystallographic axes do not change their orientation during the phase transformation. The angle between [010] and the **W** wall calculated from lattice constants is 27.73° , in excellent agreement with the optical observation. The angles between the walls **W** and **W'** are 85.35 and 150.11° , those between two **W** walls 55.46° and between two **W'** walls 64.76° (Fig. 9).

Optical birefringence and DTA

The temperature dependence of the optical birefringence of $\text{Pb}_3(\text{PO}_4)_2$ has been determined by Torres *et al.* (1974). By comparison of their results with the critical stress as determined by von Hodenberg & Salje (1977) it has been concluded that the optical birefringence in the cleavage plane (100) is due to the spontaneous strain by the internal elasto-optic effect.

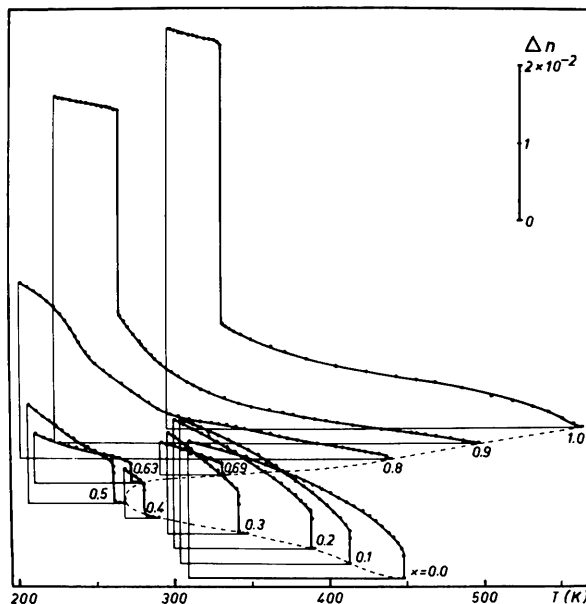


Fig. 10. Temperature dependence of the double refraction Δn for different chemical compositions. The phase transition temperatures are connected by the dashed line.

Hence the temperature dependence of the coercive stress can be determined by measurements of the spontaneous double refraction $n_b - n_c$. The experiments were performed with a high/low temperature polarization microscope and a quartz comparator. A Na lamp served as light source.

The results (Fig. 10) are in good accord with those of Torres *et al.* (1974) for $\text{Pb}_3(\text{PO}_4)_2$. All crystals with low As content show a nearly Curie-Weiss dependence of Δn on temperature and a sudden decrease by Δn_0 at or near the transition point. With increasing As content the jump Δn_0 becomes smaller and a residual double refraction appears at higher temperatures. In $\text{Pb}_3(\text{AsO}_4)_2$ the double refraction decreases abruptly during the $c \rightarrow b$ transformation, but decreases continuously at higher temperatures. The subsequent transition $b \rightarrow a$ is not accompanied by a sharp discontinuity and hence the transition temperature is difficult to obtain.

It follows that the transformation $c \rightarrow b$ is always first order, whereas the transformation $b \rightarrow a$ approaches second-order behaviour with increasing As content. This could be confirmed by DTA measurements (Fig. 11); the transition enthalpy is high for all transformations $c \rightarrow b$ and for $b \rightarrow a$ for samples with low As content. With increasing x the transition enthalpy reduces and was found to be immeasurably small in $\text{Pb}_3(\text{AsO}_4)_2$.

The phase diagram

The transition temperatures $b-c$ could easily be determined, those of the $a-b$ transformation only for low x . In other compounds, two features are used as indicators for the phase transformation: the jump of the birefringence and the (partly extrapolated) temperature with null birefringence. The latter is identical with the point of vanishing spontaneous strains. Therefore this temperature was taken as the true transition temperature (full line in Fig. 12), whereas the former indicates the jump temperature of the accompanying first-order transformation (dashed line in Fig. 12). The exact transition temperatures depend somewhat on the crystal size. Upon heating the probes from low

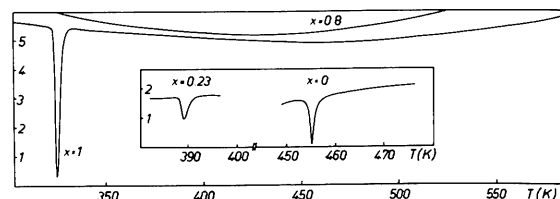


Fig. 11. DTA spectra of $\text{Pb}_3(\text{AsO}_4)_2$ ($\Delta H_{c-b} = 2.25 \text{ J g}^{-1}$), $\text{Pb}_3(\text{PO}_4)_2$ ($\Delta H_{b-a} = 0.74 \text{ J g}^{-1}$) and $\text{Pb}_3(\text{P}_{0.77}\text{As}_{0.23}\text{O}_4)_2$ ($\Delta H_{b-a} = 0.69 \text{ J g}^{-1}$).

temperatures, the fine crystalline powders transform *ca* 20 K earlier than single crystals; multidomain crystals give transition temperatures in-between. The temperatures in Fig. 12 refer to single-crystal data.

Discussion

The free energy of $\text{Pb}_3(\text{PO}_4)_2$ near the transition point can be written (Chapelle, Cao Xuan An & Benoit, 1976)

$$F = \frac{1}{2}aQ^2 + \frac{1}{4}b'Q^4 + \frac{1}{6}cQ^6$$

with

$$\frac{1}{4}b' = \frac{1}{4}b + \left(\frac{1}{2}C_{22}A + \frac{1}{2}C_{33}B + 2C_{55}C - C_{12}D + C_{23}E + 2C_{25}G\right) - \kappa$$

including the elastic energy (in brackets) and the coupling constant κ between the soft mode of A_g type and the strains ε_{ik} . This interaction energy contains linear combinations of strains and quadratic terms of the order parameter. Consequently, the spontaneous strains and Q are related by

$$\varepsilon_{ik}^0 = \alpha_{ik} Q^2.$$

These relations remain valid for all mixed crystals, whereas the order-parameter equation contains special assumptions on the elastic constants which may not hold for compounds with high As content.

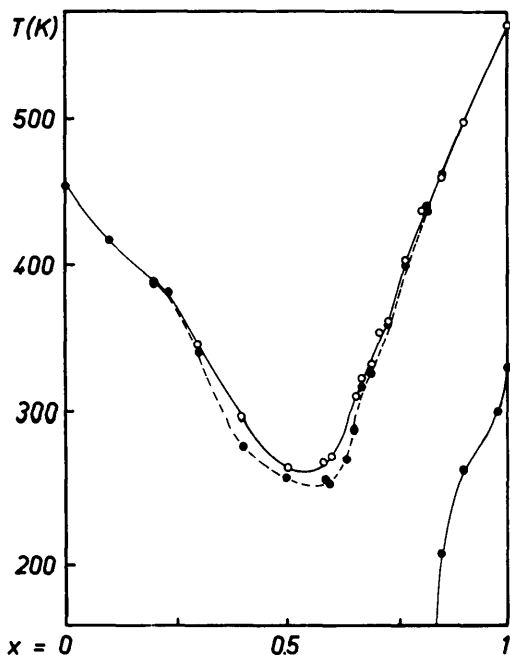


Fig. 12. Phase diagram of $\text{Pb}_3(\text{P}_{1-x}\text{As}_x\text{O}_4)_2$. The transition temperatures (full line) are for some compounds above the jump temperatures (dashed line).

In ordinary Landau theory the following relations are expected

$$\omega \simeq (T - T_c)^{\nu/2}$$

with soft-mode frequency ω and

$$\Delta S \simeq \varepsilon_{ik}^0$$

with entropy change ΔS . Gilletta, Chabin & Cao Xuan An (1976) determined ΔS in $\text{Pb}_3(\text{PO}_4)_2$ and found a quadratic dependence on temperature between 420 and 450 K. Guimaraes (1979*a*) also reported a quadratic temperature law for ε_s , although with different regimes below and above 433 K. Therefore, a critical exponent $\beta = \frac{1}{4}$ appears in contrast to most displacive transitions ($\beta = \frac{1}{2}$). Furthermore, the Curie temperature T_c appears well *below* the transition point T_0 of the high-temperature regime with $\beta = \frac{1}{2}$. These results are now confirmed for mixed crystals with the extension that the range $T_0 - T_c$ increases with increasing As content.

The critical exponent $\beta = \frac{1}{4}$ has been explained (Guimaraes, 1979*a,b*) by the assumption of $b' = 0$ below 430 K. Accordingly, the first-order behaviour in $\text{Pb}_3(\text{PO}_4)_2$ is caused by slight reductions of $b' \simeq 0$ near T_c . In $\text{Pb}_3(\text{AsO}_4)_2$ a corresponding increase of b' gives a second-order transformation ($b' \geq 0$). The result $\beta = \frac{1}{4}$ is also in accordance with measurements of the coercive stress (von Hodenberg & Salje, 1977).

In contrast to these results different critical parameters of the soft modes were derived from neutron scattering experiments. As Joffrin *et al.* (1979) report, the temperature dependence of the squared soft-mode frequency is

$$\omega^2 \simeq (T - T_0)^\nu$$

with

$$\begin{aligned} \gamma &\simeq 1.0 & T < 433 \text{ K} & & T_0 &\simeq 473 \text{ K} \\ \gamma &\simeq 1.7 & 453 < T < 573 \text{ K} & & T_0 &= 458 \text{ K} \\ \gamma &\simeq 1.0 & T > 573 \text{ K} & & T_0 &= 443 \text{ K}. \end{aligned}$$

The Curie temperatures are well within the respective *other* phase. It follows that the order-parameter exponent is nearly double the γ values and that the different Curie temperatures are different for the macroscopic parameters and the soft mode in phase b. One possible explanation is that the true driving soft mode of phase b has not yet been observed. Joffrin *et al.* (1979) give evidence for the existence of such an additional mode. We searched unsuccessfully for such a soft mode by Raman spectroscopy in the mixed crystals.

The critical behaviour ($b' \simeq 0$) is always accompanied by large order-parameter fluctuations near the transition point. The correlation length is expected to be large compared with the characteristic interaction radius. Although the $\text{Pb}_1\text{-Pb}_2$ deviation along the

monoclinic binary axes in phase b is mainly controlled by long-range Coulomb interactions (Salje & Iishi, 1977) this is not true for the accompanying tilts of PO_4 groups. The critical temperature range (slow motion regime) is therefore larger than, for example, in SrTiO_3 (Müller & Berlinger, 1971). The correlation time of crystal field fluctuations was found to be greater than 10^{-8} s between 448 and 453 K (Razeghi & Houlier, 1978). Accordingly, phonon modes are overdamped in neutron scattering (Joffrin *et al.*, 1979) and infrared experiments (Luspin, Servoin & Gervais, 1979). Guimaraes (1979b) found highly anisotropic B factors in X-ray experiments, and the retarded splitting of Raman and infrared lines (Benoit, 1976) is probably also due to long-range fluctuations with extremely long relaxation times. From the given experimental results, the temperature range of the fluctuation regime is larger in $\text{Pb}_3(\text{AsO}_4)_2$ and some mixed crystals than in $\text{Pb}_3(\text{PO}_4)_2$. We therefore propose neutron scattering experiments, similar to those performed by Joffrin *et al.* (1979) on crystals with $x \gtrsim 0.6$, where the thermal range of order-parameter fluctuations is enhanced compared with $\text{Pb}_3(\text{PO}_4)_2$.

Note added in proof: While this paper was in the press Dr Glazer informed us about the recent results of Wood, Wadhawan & Glazer (1981) concerning the temperature dependence of the optical birefringence of $\text{Pb}_3(\text{PO}_4)_2$. Their experimental results are in very good agreement with those shown in Fig. 10, $x = 0$. Their critical exponent $\beta = \frac{1}{4}$ for temperatures sufficiently below T_0 is identical with ours. It is noteworthy that the regime with $\beta = \frac{1}{2}$ near T_0 appears just for $\text{Pb}_3(\text{PO}_4)_2$ but not for all the quaternary oxides.

We are grateful to Dr Glazer for this information and for helpful discussion.

Acta Cryst. (1981). **A37**, 153–162

The Effect of Data Truncation on the Measurability of Bijvoet Differences

BY S. PARTHASARATHY AND M. N. PONNUSWAMY

Department of Crystallography and Biophysics, University of Madras, Guindy Campus, Madras-600025, India*

(Received 1 April 1980; accepted 13 May 1980)

Abstract

Theoretical expressions for the complementary cumulative function of the Bijvoet ratio X applicable to a

* Contribution No. 518.

References

- AIZU, K. (1970). *J. Phys. Soc. Jpn*, **28**, 706–716.
 BENOIT, J. P. (1976). *Ferroelectrics*, **13**, 331–332.
 BENOIT, J. P. & CHAPPELLE, J. P. (1974). *Solid State Commun.* **15**, 531–533.
 BRIXNER, L. P., BIERSTEDT, P. E. & JAEP, W. F. (1973). *Mater. Res. Bull.* **8**, 497–504.
 CHABIN, M. & GILLETTA, F. (1977). *J. Appl. Cryst.* **10**, 247–251.
 CHAPPELLE, J. P., CAO XUAN AN & BENOIT, J. P. (1976). *Solid State Commun.* **19**, 573–575.
 DECKER, D. L., PETERSEN, S., DEBRAY, D. & LAMBERT, M. (1979). *Phys. Rev. B*, **19**, 3552–3555.
 GILLETTA, F., CHABIN, M. & CAO XUAN AN (1976). *Phys. Status Solidi A*, **35**, 545–549.
 GUIMARAES, D. M. C. (1979a). *Phase Transitions*, **1**, 143–154.
 GUIMARAES, D. M. C. (1979b). *Acta Cryst.* **A35**, 108–114.
 HODENBERG, R. VON (1974). *Ber. Dtsch. Keram. Ges.* **51**, 64–68.
 HODENBERG, R. VON & SALJE, E. (1977). *Mater. Res. Bull.* **12**, 1029–1034.
 JOFFRIN, C., BENOIT, J. P., CURRANT, R. & LAMBERT, M. (1979). *J. Phys. (Paris)*, **40**, 1185–1195.
 JOFFRIN, C., BENOIT, J. P., DESCHAMPS, L. & LAMBERT, M. (1977). *J. Phys. (Paris)*, **38**, 205–213.
 LUSPIN, Y., SERVOIN, J. L. & GERVAIS, F. (1979). *J. Phys. Chem. Solids*, **40**, 661–668.
 MÜLLER, K. A. & BERLINGER, W. (1971). *Phys. Rev. Lett.* **26**, 13–16.
 RAZEGHI, M. & HOULIER, B. (1978). *Phys. Status Solidi B*, **89**, K135–K137.
 SALJE, E. & HOPPMANN, G. (1976). *Mater. Res. Bull.* **11**, 1545–1550.
 SALJE, E. & IISHI, K. (1977). *Acta Cryst.* **A33**, 399–408.
 TOLEDANO, J. C., PATEAU, L., PRIMOT, J., AUBRÉE, J. & MORIN, D. (1975). *Mater. Res. Bull.* **10**, 103–112.
 TORRES, J. (1975). *Phys. Status Solidi B*, **71**, 141–150.
 TORRES, J., AUBRÉE, J. & BRANDOU, J. (1974). *Opt. Commun.* **12**, 416–417.
 WOOD, I. G., WADHAWAN, V. K. & GLAZER, A. M. (1981). *J. Phys. C*. In the press.

truncated data set are worked out for a non-centrosymmetric crystal containing P anomalous scatterers in the unit cell [$P = 1$ and many (MN and MC cases)] besides a large number of normal scatterers. These expressions contain the truncation limit y_t as a parameter of the distribution. The results obtained are